Electronic Supplementary Information

Single Transition atom-doped Antimonene as Highly Efficient Electrocatalysts for the Nitrogen Reduction Reaction: a DFT study

Xiaopeng Shen*[a], Chao Liu[b], Qinfang Zhang*[c]

[a]*Department of Chemistry and Chemical Engineering, Yancheng Institute of Technology, Yancheng, Jiangsu 224051, P. R. China*

[b]*School of Materials Science and Engineering, Yancheng Institute of Technology, Yancheng 224051, PR China*

[c]*Key Laboratory for Ecological-Environment Materials of Jiangsu Province, Yancheng Institute of Technology, Yancheng 224051, PR China*

*To whom correspondence should be addressed. Email: shenxpeng@ycit.edu.cn (X.Shen), qfangzhang@gmail.com (Q. Zhang)

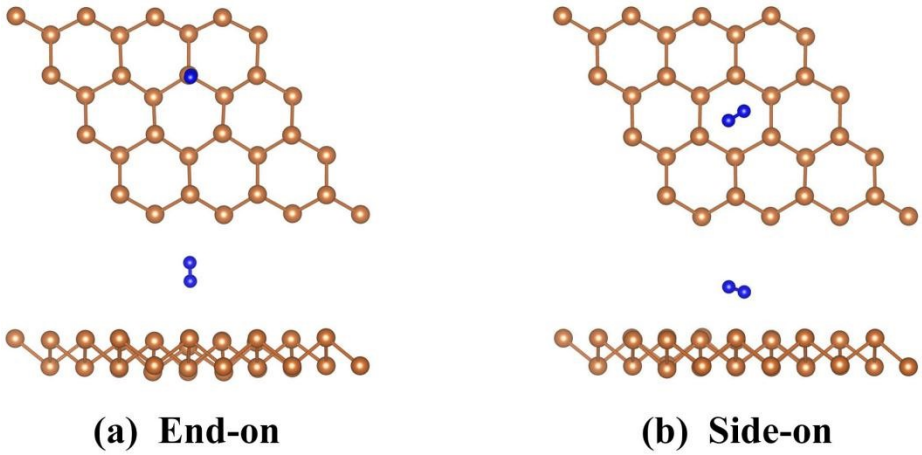

Figure S1. Top and side view of the optimized geometric structures of the adsorption of N_2 on pristine SbML by the (a) end-on and (b) side-on patterns.

Table S1. Calculated adsorption energies values of N_2 on pristine SbML by the end-on and side-on patterns .

Systems	Adsorption energies (eV)	N-N bond lengths (Å)	N-Sb distances (Å)
pristine SbML@N_2 end-on	4.21	1.11	3.91
pristine SbML@N_2 side-on	4.19	1.11	3.71

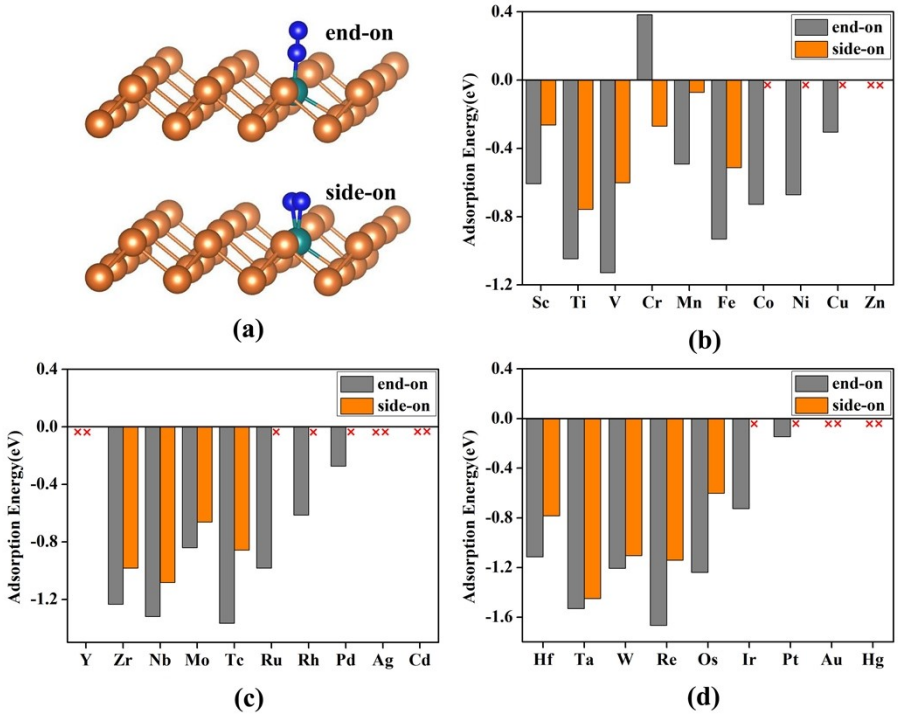

Figure S2. (a) The geometric structures of the adsorption of N_2 on defective SbML via the end-on and side-on configures. Adsorption energy (E_{ads} in eV) of N_2 adsorbed on (b) 3d TM@SbML, (c) 4d TM@SbML and (d) 5d TM@SbML.

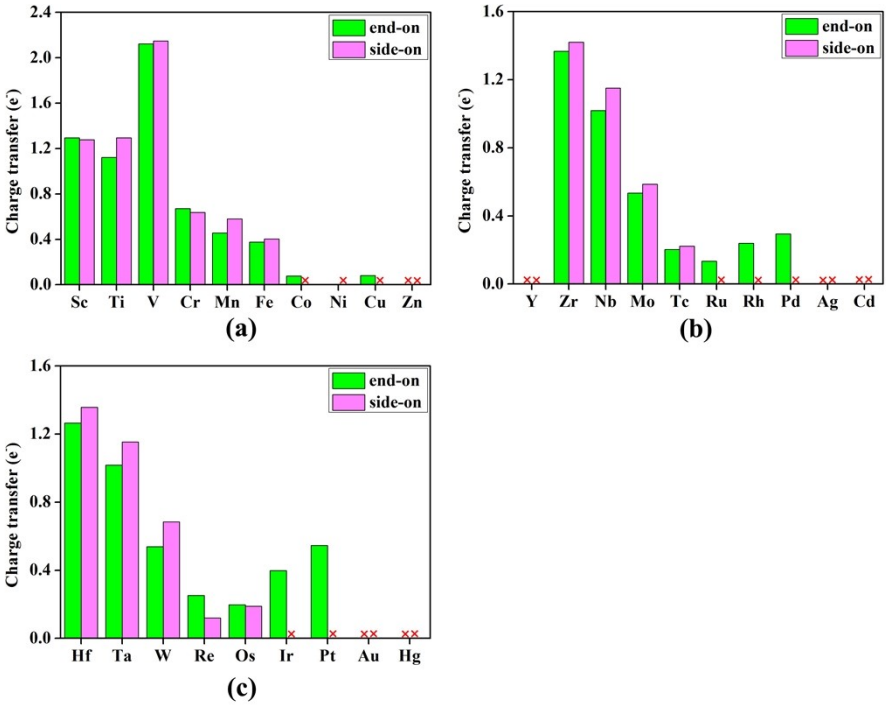

Figure S3. Bader charge transfer of (a) 3d , (b) 4d and (c) 5d TM atoms on defective SbML with N_2 end-on and side-on adsorption configures.

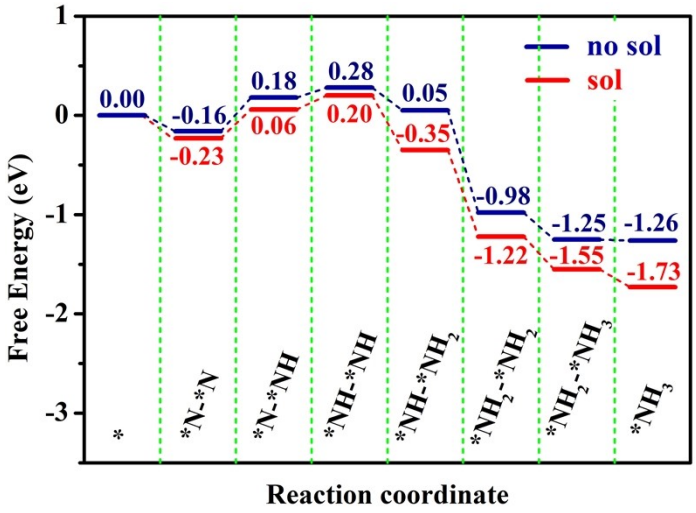

Figure S4. Gibbs free energy diagrams of NRR processes without/with solvent effect along the enzymatic pathways on Mo@SbML.

Table S2. The limiting potential values (U_L) of PDS for NRR on Mo@SbML without and with solvent effect.

Catalysts	without solvent effect (V)	with solvent effect (V)
Mo@SbML	-0.34	-0.29

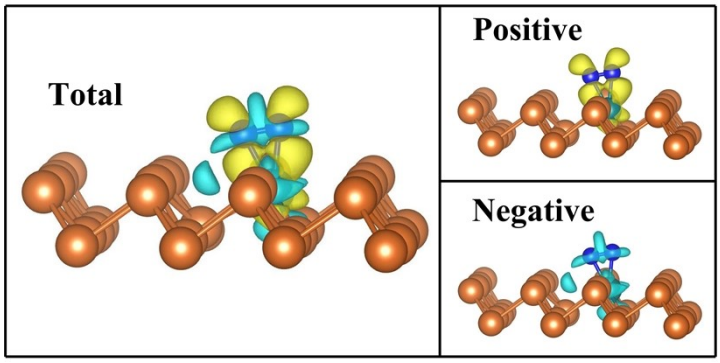

Figure S5. The charge density difference maps of the optimized structures of N_2 adsorbed on Mo@SbML with side-on configuration, where the isosurface value is set to be 0.0013 e Å^{-3} and the positive and negative charges are shown in yellow and cyan, respectively.

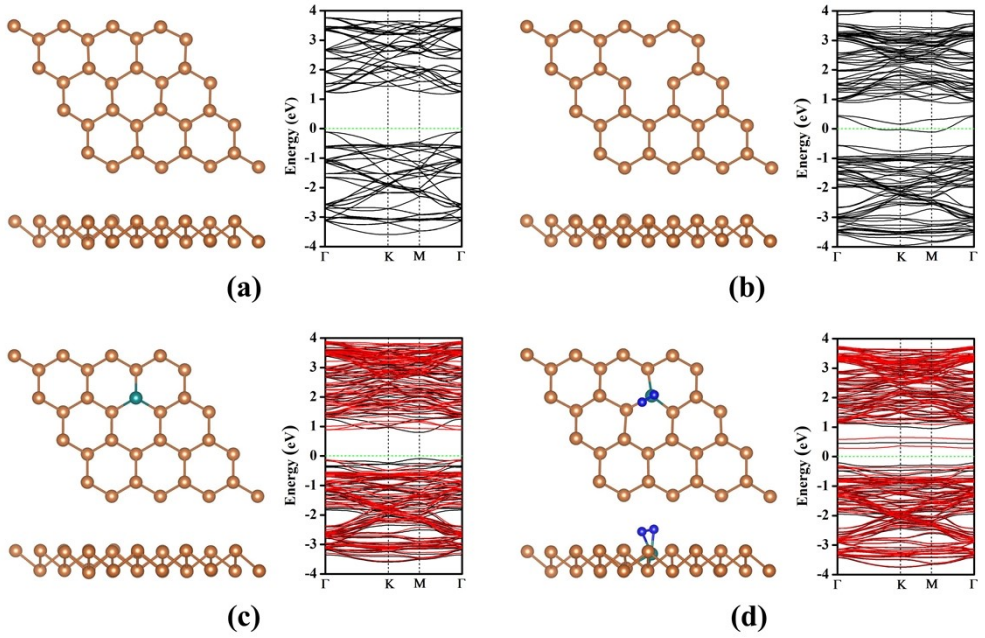

Figure S6. The pristine antimonene monolayer (a), defective SbML with Sb monovacancy (b), Mo@SbML (c) and N_2 adsorption on Mo@SbML with side-on configuration (d) of top view and side view, and the corresponding band structures (DFT-PBE level). The black and red dotted lines in the band structures denote the spin-up (↑) and spin-down (↓) channels, respectively. The Fermi-level is set to be zero denoted by green dash line. The green color is represented for arsenic atom. The orange, blue, and cyan denote Sb, N, and Mo atoms, respectively.

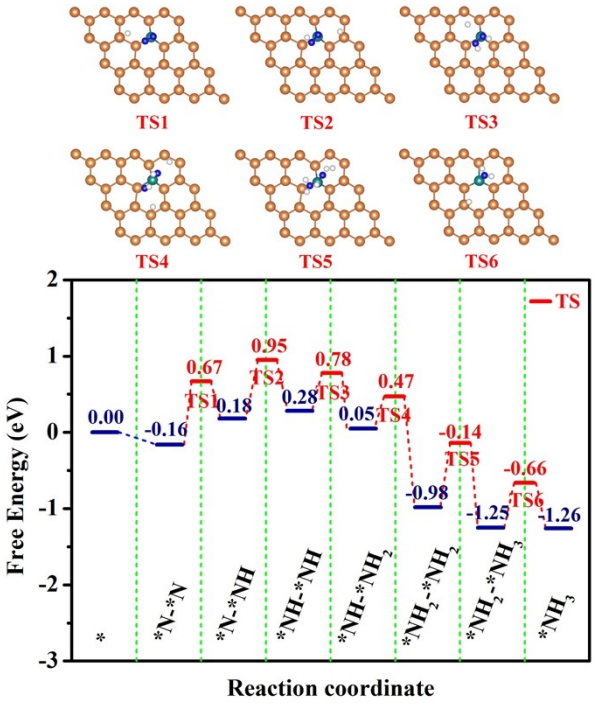

Figure S7. Minimum energy path for the entire NRR process on the Mo@SbML surface. The corresponding structures of intermediates and transition states are labeled.

Table S3. The integrated COHP (ICOHP) value (eV) between N–N of free N_2 molecule, N_2 adsorbed on different catalyst with side-on configuration and end-on configuration and the corresponding limiting potential (U_L) (eV).

Catalyst	integrated COHP (ICOHP) value (eV)			limiting potential (U_L) (eV)	Ref.
	free N_2	side-on configuration	end-on configuration		
Mo@SbML	-23.52	-8.89	-10.28	-0.34	this work
Cr@GY	-22.98	-19.39	-22.25	-0.52	44
Mn@GY	-22.98	\	-22.10	-0.36	36
V@GY	-22.98	-21.08	\	-0.60	36
Ta@g-C_7N_3	-11.46	\	-7.18	-0.27	47

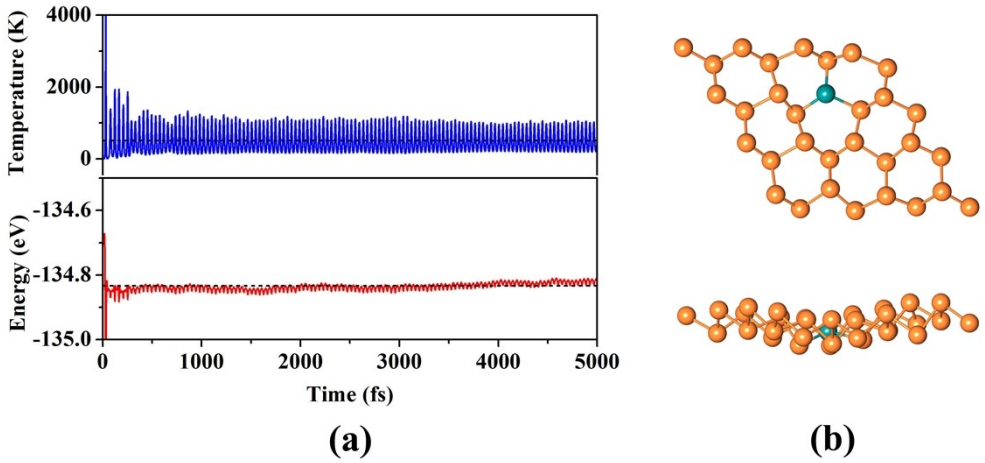

Figure S8. (a) The temperature and energy fluctuations of Mo@SbML during 5 ps of AIMD simulation with a time step of 1 fs. (b) The top and side views of Mo@SbML after 5 ps of AIMD simulation at T = 500 K.